electricity

MDPI

Article

Peak Shaving with Battery Energy Storage Systems in Distribution Grids: A Novel Approach to Reduce Local and Global Peak Loads

Daniel Kucevic *, Leo Semmelmann, Nils Collath, Andreas Jossen and Holger Hesse

Institute for Electrical Energy Storage Technology, School of Engineering and Design, Technical University of Munich (TUM), 80333 Munich, Germany; leo.semmelmann@tum.de (L.S.); nils.collath@tum.de (N.C.); andreas.jossen@tum.de (A.J.); holger.hesse@tum.de (H.H.)

* Correspondence: daniel.kucevic@tum.de

Abstract: The growing global electricity demand and the upcoming integration of charging options for electric vehicles is creating challenges for power grids, such as line over loading. With continuously falling costs for lithium-ion batteries, storage systems represent an alternative to conventional grid reinforcement. This paper proposes an operation strategy for battery energy storage systems, targeted at industrial consumers to achieve both an improvement in the distribution grid and electricity bill savings for the industrial consumer. The objective is to reduce the peak power at the point of common coupling in existing distribution grids by adapting the control of the battery energy storage system at individual industrial consumer sites. An open-source simulation tool, which enables a realistic simulation of the effects of storage systems in different operating modes on the distribution grid, has been adapted as part of this work. Further information on the additional stress on the storage system is derived from a detailed analysis based on six key characteristics. The results show that, with the combined approach, both the local peak load and the global peak load can be reduced, while the stress on the energy storage is not significantly increased. The peak load at the point of common coupling is reduced by 5.6 kVA to 56.7 kVA and the additional stress for the storage system is, on average, for a six month simulation, period only 1.2 full equivalent cycles higher.

Keywords: battery energy storage system; lithium-ion; grid-integrated energy storage; peak shaving; distribution grid; peak load reduction

Citation: Kucevic, D.; Semmelmann, L.; Collath, N.; Jossen, A.; Hesse, H. Peak Shaving with Battery Energy Storage Systems in Distribution Grids: A Novel Approach to Reduce Local and Global Peak Loads. *Electricity* **2021**, *2*, 573–589. https://doi.org/10.3390/electricity2040033

Academic Editor: Andreas Sumper

Received: 28 September 2021
Accepted: 4 November 2021
Published: 15 November 2021

1. Introduction

The steadily increasing demand for electrical energy is leading to new challenges for the power grid [1]. The grid infrastructure must be tailored to tolerate the peak load conditions and grid operators must ensure this [2]. Conventional grid reinforcement or transformer upgrading, as investigated by Brinkel et al., is one possible solution for covering the increasing demand or to enable the integration of more electric vehicles [3]. However, with falling costs of lithium-ion batteries (LIBs), stationary battery energy storage systems (BESSs) are becoming increasingly attractive as an alternative method to reduce peak loads [4,5].

The peak shaving field has seen an increasing interest in research during the last years. Oudalov et al. were among the first to introduce a BESS sizing methodology and operation strategy to reduce the peak load of an industrial customer, thereby reducing its total electricity bill. Since grid operators in many jurisdictions charge large-scale consumers for their highest power demand, it can be economically viable to install a BESS and discharge it when a certain power threshold is surpassed. The objective for optimal BESS operation is to maximize the profit of the peak shaving operations with respect to the shaved power, battery cycles per year, battery lifetime, and the power demand fee. The optimal trajectory of BESS charging and discharging events-resulting from the peak

shaving operating strategy-is retrieved through dynamic programming. In their work, electricity bill reduction to the amount of 8% was reached through a lead-acid based BESS. However, in this study the focus was on the optimization of the BESS and the economic effects and not on the possible grid relief achievements through the peak shaving strategy on the distribution grid. [6]

In the study of Mamun et al. the management of a lithium-ion based BESS was optimized in order to maximize peak shaving-induced electricity bill savings while minimizing battery degradation [7]. The focus here was on modeling the battery degradation mechanisms and the economic benefits and again not on the effects on the distribution grid. In the study of Tiemann et al. a large-scale peak shaving profitability analysis of more than 5300 industrial customer load profiles in Germany was conducted [8]. The authors also came to the conclusion that the peak shaving technology yields the highest profits, compared to other battery use cases. Furthermore, the authors state that in many cases minimal payback periods for peak shaving operations can be reached. This is supported by the work of Martins et al., who concluded that peak shaving is already profitable in many cases for industrial customers in Germany [9].

While most peak shaving related works are focused on industrial end-customer use cases, some recent works also highlight the possible benefits of the approach for the grid. For instance, in the work of Danish et al. a BESS located in a distribution grid was optimized in order to find the optimal size, location, and control strategy. The work was based on a 20 kV distribution grid in Kabul with 22 buses and the authors have concluded that an optimally placed BESS with a peak shaving operation strategy can significantly improve the system performance and power losses can be reduced up to 20.62% [10].

However, none of these studies investigated the effects of multiple BESSs located at various industrial consumers, including accurate co-simulations of both a BESS and a distribution grid. Furthermore, the potential of coupled energy management strategies has not yet been analyzed in order to achieve both an improvement in the distribution grid as well as electricity bill savings for industrial consumers.

1.1. Scope of the Study

This study shows different operation strategies for a number of stand-alone BESSs to reduce the local peak load (Strategy α) or the peak load at the point of common coupling (β) or both (γ). The BESSs located at various nodes in an example grid are economically optimal sized using a linear programming approach. First, these storage systems are operated with a state-of-the-art peak shaving strategy. In the second step, the identically sized BESSs are used and a centralized control approach is chosen to reduce the peak load at the point of common coupling (PCC). Finally, in a new approach introduced in this study, these two approaches are combined in order to achieve both a local and a global peak load reduction. This scope of the study is condensed as a graphical overview in Figure 1. The paper can be summarized as follows:

- With accurate co-simulations of BESSs and distribution grids, results for various operation strategies aiming to reduce both the local peak load and the global peak load are acquired.
- The storage systems are economical optimally sized using linear optimization.
- These storage systems are operated with a state-of-the-art peak shaving strategy as well as with a centralized approach and compared according to the peak load reduction at a specific node and the PCC.
- A newly combined approach is developed aimed to reduce the peak power at the PCC in an example distribution grid while not significantly influencing the peak load reduction for the individual industrial consumer.
- The stress on the storage system for the various operation strategies is derived from a detailed analysis based on six key characteristics.

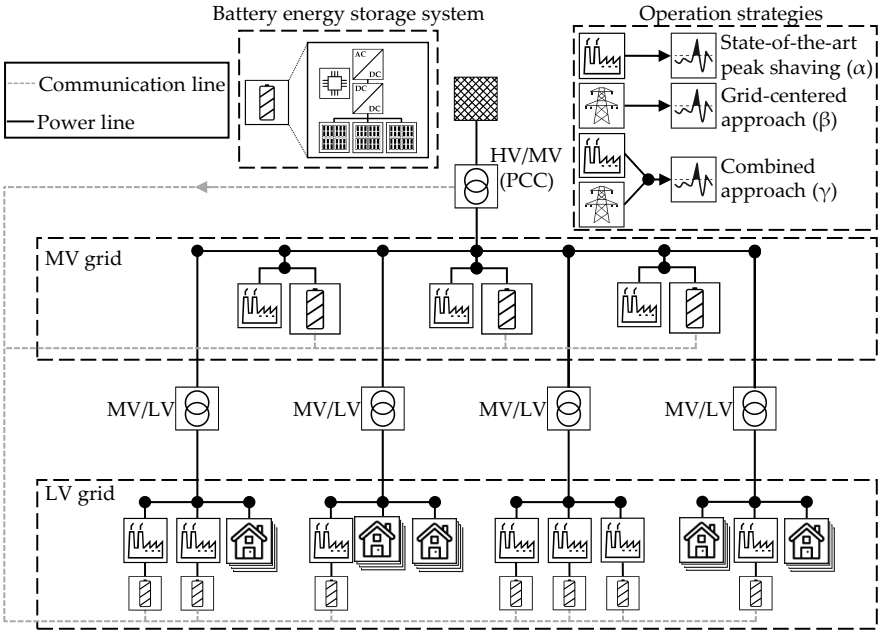

Figure 1. Graphical overview of the simulated grid and battery energy storage systems (BESSs), as well as the investigated operation strategies. The BESS, modeled in detail, located at various nodes in a test grid, is operated in three different operation strategies to reduce the local peak load (Strategy α) or the peak load at the point of common coupling (β) or both (γ).

1.2. Outline of the Paper

The remainder of this paper is structured as follows: Configuration of the grid and the BESS as well as the simulation settings are described in Section 2. Section 3 describes the methodology of this study, including a mathematical and graphical representation of all three energy management strategies used. The results of the simulations are presented and discussed in Section 4, while Section 5 concludes the paper with an outlook on potential directions of future work.

2. Simulation Settings and System Configurations

This section describes the simulation tools applied as well as the example grid used and the BESSs settings. To analyze the behavior and the effects on the distribution grid of storage systems, accurate simulations of BESSs and distribution grids are necessary. Figure 2 shows an overview of all simulation tools used in this work, which are all available open-source (open_BEA and SimSES: https://www.ei.tum.de/en/ees/research-teams/team-ses/system-analytics-and-integration/, accessed on 2 November 2021; eDisGo: https://github.com/openego/eDisGo, accessed on 2 November 2021). All settings, such as the selection of the grid, the simulation duration, and the operation strategy are defined within open_BEA. A further description of open_BEA can be found in [11]. In this work, open_BEA is used to analyze the effects of novel operation strategies for BESSs on the peak load at the PCC in a distribution grid.

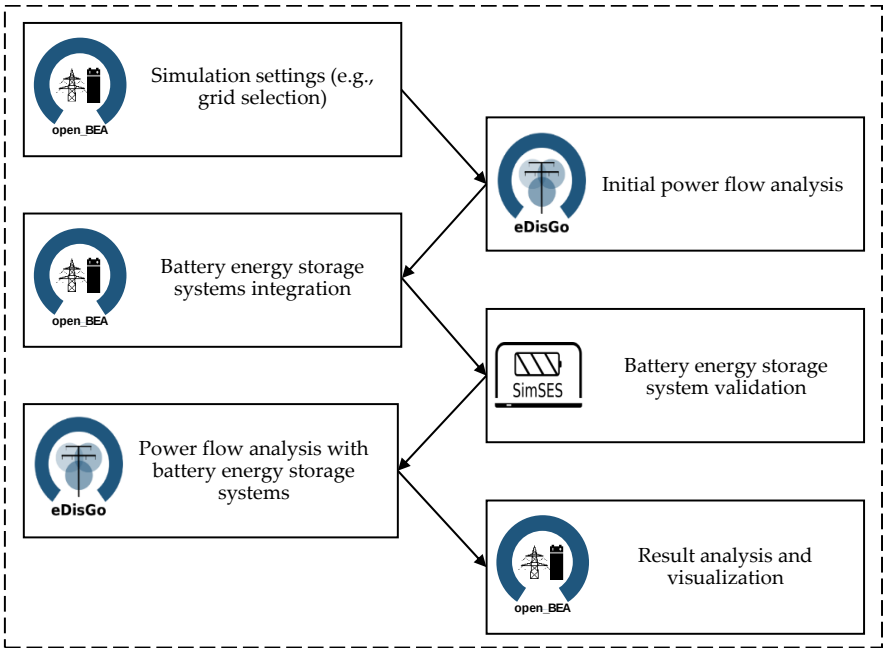

Figure 2. Overview of all open-source simulation tools, which have been adapted for use in this study. The open_BEA tool operates as both a central control unit and as a configuration unit. The eDisGo tool conducts the power flow analysis and SimSES operates as a validation unit for the battery energy storage systems' behavior.

In addition to the specification of the test grid and the operation strategies ($\alpha - \gamma$) of the BESSs, individual load demands are assigned to the various actors in the grid within open_BEA. Based on these load demands for residential or industrial consumers, the eDisGo software performs a power flow analysis for a selected period. In this step, the power flow analysis is conducted without storage systems. This allows determining the power flows at all specific nodes and lines for the entire simulation period. These power flow results as well as the power at the PCC are transferred back to open_BEA for the next simulation step. Based on the power flow results, the dis(-charging) strategy for each BESS is calculated according to the selected operation strategy (cf. Section 3).

The main task of SimSES is to validate the effects of the target power provided by the energy management system of the open_BEA tool regarding efficiency, temperature, and degradation of the BESS when applied to the storage system. Each implemented component, such as the power electronics unit or the battery type, is responsible for modeling its relevant principles [12]. SimSES can be split into a simulation part for modeling the physical behavior of the BESS and an evaluation part that provides technical results for this study. The validated BESS time series are now included in the grid and an additional power flow analysis is conducted with eDisGo and the results are fed back to open_BEA for further analysis and visualization.

2.1. Example Grid and Denotations

As our aim is to investigate the effects of various BESS strategies on the distribution grid, an example grid including an open loop medium voltage (MV)-grid with 146 underlying low voltage (LV)-grids is used. The exemplary grid is connected to the overlying grid level through a single substation (PCC). This grid was chosen because of its resemblance to the typical German grid structure [13]. A graphical representation is shown in Figure 3 in which the circuit breakers are marked in gray, the 146 MV/LV transformers in light blue, the PCC in red, and all branch tees in dark blue.

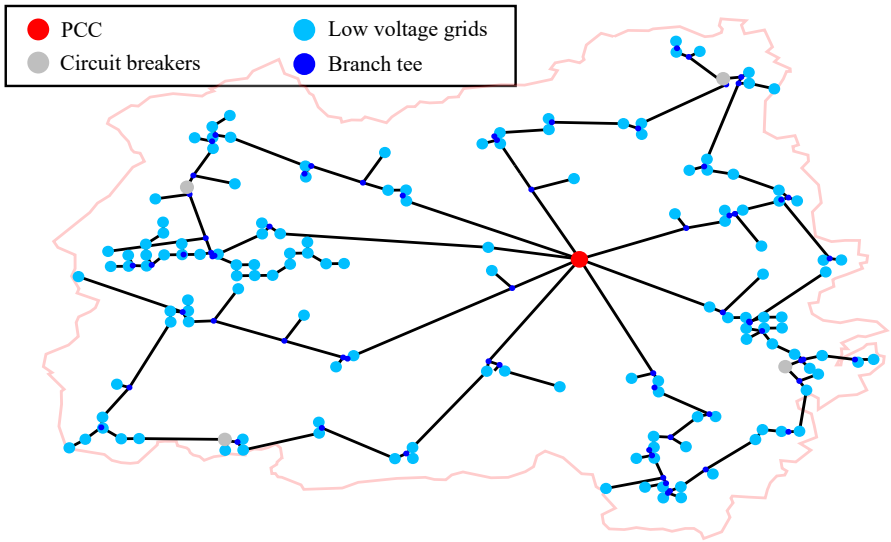

Figure 3. Graphical representation of the test distribution grid. The open circuit breakers are marked in gray, the MV/LV transformers are marked in light blue, the PCC in red, and all branch tees in dark blue.

The distribution grid includes 72 industrial consumers with an annual load above 100 MWh. Only these end-users can potentially benefit from applying peak shaving through a BESS as described in Section 3.1. Equation (1) defines the vector $\mathbf{N}$ for all industrial consumers b within the described distribution grid, with a total number of nodes B:

$$\mathbf{N} = [1, \cdots, \mathrm{b}, \cdots, \mathrm{B}]^{\mathrm{T}} \tag{1}$$

The current time step t within a defined time horizon T is defined by a vector H as shown in Equation (2):

$$\mathbf{H} = [1, \cdots, t, \cdots, \mathrm{T}] \tag{2}$$

Finally, the apparent power $\mathrm{S}_t^{\mathrm{b}}$ at each node b for each time step t is defined by a matrix $\mathbf{S}$ (Equation (3)). The individual load profiles for these industrial consumers as well as all other consumers in the grid are according to a former publication [14].

$$\mathbf{S} = \begin{pmatrix} \mathrm{S}_1^1 & \cdots & \mathrm{S}_t^1 & \cdots & \mathrm{S}_{\mathrm{T}}^1 \\ \vdots & \ddots & \vdots & \ddots & \vdots \\ \mathrm{S}_1^{\mathrm{b}} & \cdots & \mathrm{S}_t^{\mathrm{b}} & \cdots & \mathrm{S}_{\mathrm{T}}^{\mathrm{b}} \\ \vdots & \ddots & \vdots & \ddots & \vdots \\ \mathrm{S}_1^{\mathrm{B}} & \cdots & \mathrm{S}_t^{\mathrm{B}} & \cdots & \mathrm{S}_{\mathrm{T}}^{\mathrm{B}} \end{pmatrix} \tag{3}$$

2.2. Battery Energy Storage System Setting

As described in the previous section, the SimSES simulation tool is used to validate the behavior of the BESS and to obtain detailed insights of the stress of the storage system. The parameters and settings shown in Table 1 are used in this paper to represent and simulate a realistic BESS. For the battery, a LIB with a lithium-iron-phosphate (LFP) cathode and a carbon/graphite (C) anode is selected [15]. This type of cell is particularly suitable for stationary applications due to its higher cycle durability [16]. The power electronics (AC/DC converter) is modeled by a constant load-independent part and a second part, including all load-dependent losses [17]. The maximum efficiency with this converter type is attained at 0.46· P^{rated} with an efficiency of η_{PE} = 96.9%. In accordance with the type of battery cell, the maximum $\mathrm{e}^{\mathrm{rate}}$ is set to 1 h^{-1}.

Table 1. Parameters and settings of the simulated battery energy storage system (BESS) comprising battery cells, a power electronics unit, and a battery management system (BMS).

Parameter/Setting	Description/Value	Unit
Battery cell manufacturer	Murata	-
Battery cell type	US26650FTC1	-
Battery cell chemistry	LFP:C	-
Battery cell capacity	2850	mAh
Nominal cell voltage	3.2	V
Cell voltage range	2–3.6	V
Maximum efficiency of power electronics	96.9	%
Maximum e^{rate}	1	h^{-1}
Starting state of energy (SOE)	100	%

2.3. Simulation Setting

All results shown in this study are based on a simulation duration of six months, which represents a tradeoff between seasonal fluctuation and computation time, and a simulation step size of 15 min. The 15-minute time discretization is based on the fact that tariff calculations in Germany are calculated with maximum values in 15 min time step demand averages [18]. The simulation tools used in this work are implemented in Python. The linear optimization algorithm in Section 3.4 is implemented using MATLAB® programming language.

3. Problem Formulation and Applied Methods

3.1. Peak Shaving Operation Strategy: Strategy α

Motivated by a tariff system consisting of an energy demand charge and a peak power tariff, the aim of state-of-the-art peak shaving is to minimize the maximum power peak value at one specific node b within a defined billing period. The grid operator expects the use of this tariff scheme to avoid cable overloading and lower peak loads on the transformer [19].

In particular, large electricity consumers with an annual demand above a certain limit (in Germany 100 MWh [18]) can reduce the peak power provided by the power grid, which directly results in reduced operating expenses in the form of reduced grid charges. In order to reduce the peak power at a specific node b, the excess demand has to be either covered by another power providing unit, such as a diesel generator, or in our case, a BESS. The BESS is used to decouple the supply and demand over a specified time. Consequently, it is essential to find a peak shaving threshold $S^{thresh,b}$ above which the power is provided by the BESS.

In this work, we assume a straightforward charging approach as described in Equations (4) and (5): the BESS is charged whenever the apparent power S_t^b of the given load profile falls below a previously defined peak shaving threshold $S^{thresh,b}$ and discharged when the threshold is exceeded. With this strategy, the BESS is fully charged most of the time and is only used, if the local load is above the peak shaving threshold $S^{thresh,b}$. This operation mode is therefore independent of the load at the PCC and is therefore the most reliable strategy for a consumer with the only goal to reduce the local peak load. The methodology to find the peak shaving threshold $S^{thresh,b}$ is described in Section 3.4.

$$\text{Charging}: \quad S_t^b < S^{thresh,b} \quad \forall\, t \tag{4}$$

$$\text{Discharging}: \quad S_t^b > S^{thresh,b} \quad \forall\, t \tag{5}$$

3.2. Grid-Centered Peak Shaving: Strategy β

This subsection introduces an approach to use BESSs of distributed industrial customers to reduce power peaks at the grid operator's PCC. To achieve this, the vector of the

apparent power $\mathbf{S}^{\mathrm{PCC}}$ at the PCC is used to determine the operation strategy of BESSs of industrial customers instead of the local load profile vector.

$$\mathbf{S}^{\mathrm{PCC}} = \left[\mathrm{S}_1^{\mathrm{PCC}}, \cdots, \mathrm{S}_t^{\mathrm{PCC}}, \cdots, \mathrm{S}_{\mathrm{T}}^{\mathrm{PCC}}\right] \tag{6}$$

The optimization goal of grid-centered peak shaving is to minimize the peak power at the PCC instead of the power peak at a specific node b (Strategy α). Consecutively, the peak shaving thresholds of the industrial customers storage systems are recalculated in order to maximally reduce the peak power with a given BESS capacity by the previously introduced method, while $\mathbf{S}^{\mathrm{PCC}}$ serves as input for the peak shaving scheduling. The new threshold $\mathrm{S}^{\mathrm{thresh,PCC}}$ is calculated using an iterative approach [20].

3.3. Combined Peak Shaving Approach: Strategy γ

This subsection introduces an approach to use industrial customers' BESS to reduce both PCC and local peaks. First, a scaling factor σ_{b} for every node b is calculated that sets the highest PCC power in relation to the highest power at a specific node b as showed in Equation (7).

$$\sigma_{\mathrm{b}} = \frac{\max\left(\mathrm{S}_t^{\mathrm{b}}\right)}{\max\left(\mathbf{S}^{\mathrm{PCC}}\right)} \tag{7}$$

In Equation (8), every load of the vector $\mathbf{S}^{\mathrm{PCC}}$ is multiplied by σ_{b} to scale the PCC load profile down to the dimensions of the load profile at a specific node b. The scaled-down vector is denoted as $\mathbf{S}^{\mathrm{Scaled,b}}$.

$$\mathbf{S}^{\mathrm{Scaled,b}} = \mathbf{S}^{\mathrm{PCC}} \cdot \sigma_{\mathrm{b}} \tag{8}$$

Based on $\mathbf{S}^{\mathrm{Scaled,b}}$ and the local load profile $\mathbf{S}_t^{\mathrm{b}}$ at node b in Equation (9) a combined load profile $\mathrm{S}_t^{\mathrm{comb}}$ is created. For every point of time t in T, the maximum value of $\mathbf{S}^{\mathrm{Scaled,b}}$ and $\mathbf{S}^{\mathrm{b}}$ is used to obtain the combined load profile $\mathrm{S}_t^{\mathrm{comb}}$ that takes both the peaks at the PCC and the local peaks into account.

$$\mathbf{S}^{\mathrm{comb,b}} = \max(\mathbf{S}_t^{\mathrm{Scaled,b}}, \mathbf{S}_t^{\mathrm{b}}) \quad \forall t \tag{9}$$

Subsequently, $\mathrm{S}_t^{\mathrm{comb}}$ serves as the input for the peak shaving operation strategy. Again, the peak shaving thresholds of the industrial customers' storage systems are recalculated in order to maximally reduce the peak power with given capacities. The new threshold $\mathrm{S}^{\mathrm{thresh,comb}}$ is calculated using an iterative approach [20]. It must be noticed that this strategy is less reliable for the reduction of the local peak load than strategy α, since the BESS now also might be used to reduce the peak load at the PCC. However, this will be discussed in more detail in Section 4.

All three energy management strategies used in this work are depicted in Figure 4. All solid lines mark the results of the power flow analysis without BESS and the dashed lines marks the results of the power flow analysis including a BESS at a specific node b. The black solid line associated to the right y-axis shows the difference in power, covered by the BESS. In this example, a BESS with an energy content of 100 kWh is used to shave the peaks. The upper plot (a) shows the results for an exemplary industrial consumer if the BESS operates in a stand-alone peak shaving mode. While in this study the BESS works only in a real power operation, the apparent power is shown in the plot.

The solid line at subplot (b) shows the results for the power flow analysis at the PCC if the BESS at the same node b operates in a grid-centered peak shaving mode. The difference between with and without storage is very small due to the significantly higher load at the PCC compared to the load at a specific node b, so the dashed line follows the solid line almost exactly. The difference is displayed with the black solid line associated to the right y-axis. The maximum difference is with 100.2 kVA slightly higher than the maximum

power of the exemplary BESS. This is due to the fact that the BESS is placed at a specific node b and because of this, less energy has to be transmitted from the PCC to this node. This allows line losses to be reduced.

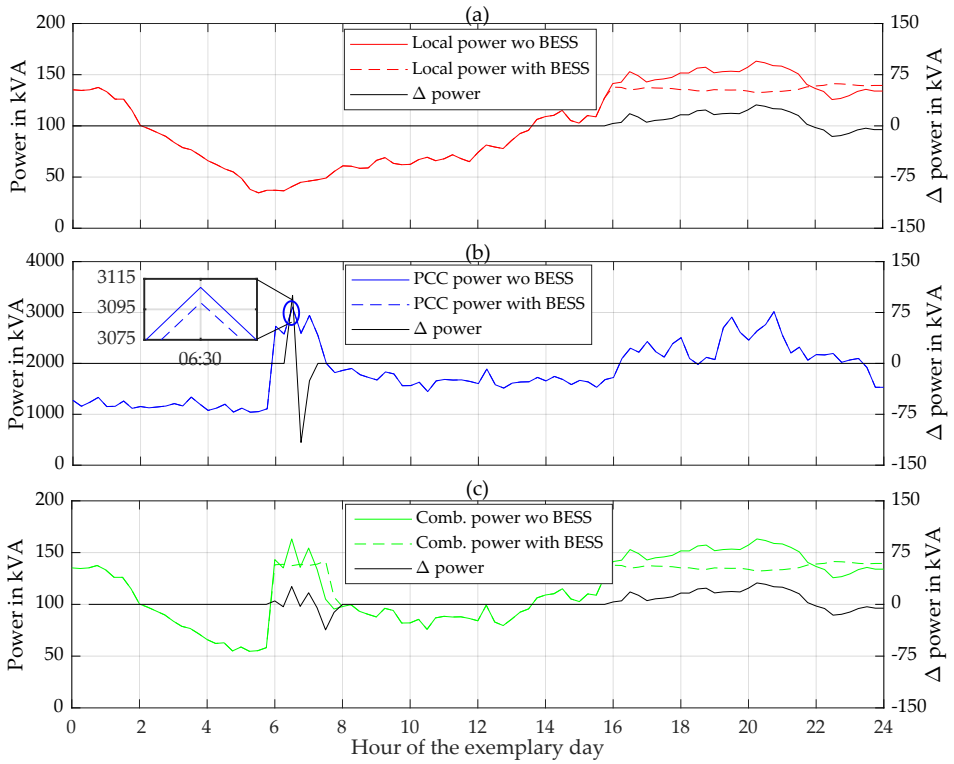

Figure 4. Graphical representation of all three energy management strategies used in this study. Subplot (**a**) shows an exemplary load profile for an industrial consumer at a specific node b. The related power at the point of common coupling is displayed in subplot (**b**) and subplot (**c**) shows the combined profile. The solid line marks the results of the power flow analysis without the battery energy storage system (BESS) at a specific node b and the dashed line marks the results of the power flow analysis including the BESS. The black solid line associated to the right y-axis shows the difference in power, covered by the BESS.

The lower plot (c) shows the combined load profile S_t^{comb} (solid line) for an exemplary industrial consumer, including the scaled load from the PCC. In the hours six to eight it can be seen that the scaled load profile from the PCC is responsible for the peak. Consequently the BESS shaves this peak and therefore ensures a lower peak load at the PCC. As with strategy α, the BESS also manages to shave the local peak between hours 16 and 22 with the combined strategy. Again the black solid line shows the difference in power, covered by the BESS. Compared to the other two strategies, the BESS is stressed twice on this exemplary day. The effects of this are discussed in the next chapter.

3.4. Battery Energy Storage System: Component Sizing

Sizing of the BESSs is conducted using an adopted version of a previously described linear programming optimization approach [9]: The cost function (Equation (10)) allows finding a profit optimal compromise between electricity costs (tariff dominated by annual peak cost) as well as storage investment costs and a battery charge throughput penalty cost. Motivating low cycle counts and thus manageable cyclic aging within the project operation period, the throughput penalty cost (w_{tp}) are included and multiplied with the energy throughput ($BESS_{tp}$) of a BESS.

$$\mathrm{OBJ} = \mathrm{S}^{\mathrm{thresh,b}} \cdot \mathrm{p}_{\mathrm{peak}} \cdot \mathrm{t}_{\mathrm{proj}} + P_{max} \cdot \mathrm{e}^{\mathrm{rate}} \cdot \mathrm{p}_{\mathrm{BESS}}^{\mathrm{invest}} + BEES_{tp} \cdot w_{tp} \quad (10)$$

We choose a parameter set as follows: The storage investment costs p_{BESS}^{invest} are set to 350 $\frac{\$}{kWh}$ as motivated by [21]. A project operation/depreciation period of t_{proj}= 10 years well covered by BESS-assisted peak shaving analysis studies presented by Martins et al. [9] as well as degradation studies with the LFP:C battery cell is used herein [16,22].

In accordance with publicly available tariff tables provided by various distribution grids in Germany, a peak demand charge of $p_{peak} = 110 \frac{\$}{kVA \cdot a}$ was chosen. The e^{rate} has been set to $1\,h^{-1}$ as described in Section 2.2. For the lithium-ion based BESS investigated herein, we chose a value of unity for the this parameter yielding a well-balanced system layout and shaving of distinguished power peaks. Battery cycling and energy throughput is penalized using a weighting factor of w_{tp}= 0.001 $\frac{\$}{kWh}$ in order that the BESS is not dis(-charging) needlessly [23].

The boundary conditions of the BESS are described in the constraints Equations (11)–(15). The actual energy content for a specific time step t of a BESS, denoted as $E_t^{actual,b}$, must remain within the physical bounds of a storage system:

$$0 \cdot E^{nominal} \leq E_t^{actual,b} \leq 1 \cdot E^{nominal} \tag{11}$$

The charging and discharging powers ($P_t^{charge,b}$ and $P_t^{discharge,b}$) has to be lower than the rated power P^{rated} of the power electronics.

$$P_t^{charge,b} \leq P^{rated} \quad \forall\, b \tag{12}$$

$$P_t^{discharge,b} \geq -P^{rated} \quad \forall\, b \tag{13}$$

The charging and discharging power ($P_t^{charge,b}$ and $P_t^{discharge,b}$) for each step t and each BESS is also limited by the respective maximum energy rate (e^{rate}) of the storage system.

$$P_t^{charge,b} \leq e^{rate} \cdot E^{nominal} \quad \forall\, b \tag{14}$$

$$P_t^{discharge} \geq -e^{rate} \cdot E^{nominal} \quad \forall\, b \tag{15}$$

The actual energy content $E_t^{actual,b}$ of a BESS is calculated by adding the net charged energy $E_t^{charge,b}$ to the energy content of the previous time step and subtracting the discharged energy $E_t^{discharge,b}$. This energy conservation equation of a BESS is defined in Equation (16).

$$E_t^{actual,b} = E_{t-1}^{actual,b} + E_t^{charge,b} - E_t^{discharge,b} \tag{16}$$

In order to derive the best-suited BESS system sizing, we have applied this formulation (minimize (OBJ)) to the entire set of 72 scenarios. The linear optimization results in BESSs capacities of less than 10 kWh for 40 out of the 72 customers. These small storage sizes are neglected in this study, because the capacity is more in the range of home energy storage systems and no longer in the range of industrial storage systems [24]. The cost assumptions for the initial costs p_{BESS}^{invest} are therefore no longer valid. Furthermore, the peak load reduction and thus the cost savings would be minor in these cases and therefore are not considered further. Figure 5 visualizes relative peak shaving limits $S^{thresh,b}$ in % for all 32 BESS with a capacity above 10 kWh. The lower plot (b) shows the capacity for just these BESS.

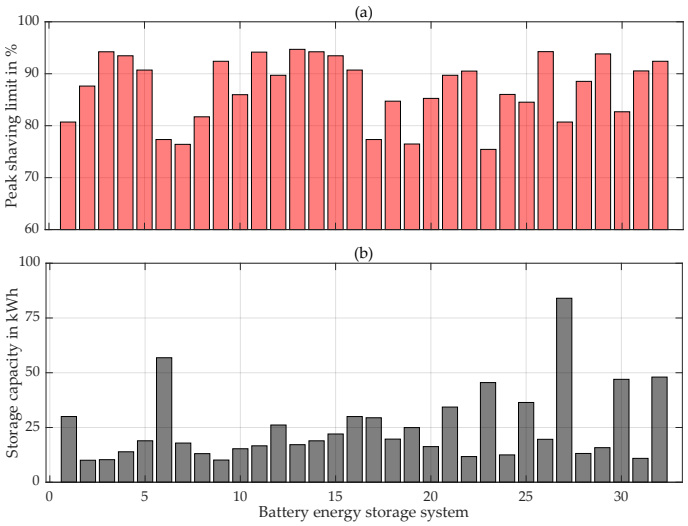

Figure 5. Results of the component sizing optimization. The upper plot (**a**) shows the peak shaving limits $S^{thresh,b}$ in % of the original peak power for all 32 battery energy storage system (BESS) with a capacity above 10 kWh. The lower plot (**b**) shows the capacity for just these BESS.

4. Case Studies and Discussion

This section discusses the impact of various strategies of storage systems on the test distribution grid for a six months simulation period. For this purpose, the load flows and potential reductions in peak load at the PCC are evaluated in detail and compared to the results obtained with a state-of-the-art peak shaving algorithm (Strategy α). The effects of these strategies as well as the resulting stress on the BESS are also investigated.

Figure 6 shows the relative peak load reduction for each of the 32 simulations with various operating strategies for the BESS. The reduction of the peak load at the local node b (= location of the BESS) is plotted on the abscissa and the reduction of the peak load at the PCC can be seen on the ordinate. The results are each related to the maximum power of the storage system. Based on an e^{rate} of 1 as defined in Section 2.2, the maximum power in kW is equal to the capacity of each BESS in kWh.

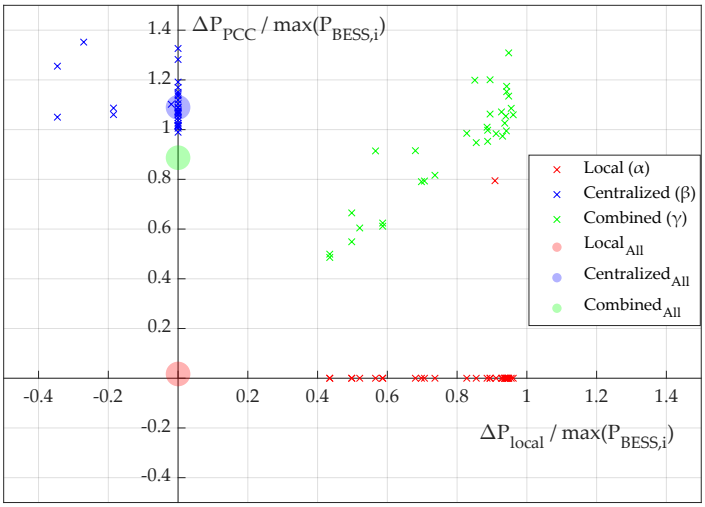

Figure 6. Relative peak load reduction for each simulation with various operating strategies for the battery energy storage system (BESS). The reduction of the peak load at the local node b (= location of the BESS) is plotted on the abscissa and the reduction of the peak load at the point of common coupling (PCC) can be seen on the ordinate. The red crosses show the reduction if the BESS is operated with strategy α. The blue crosses show the results for strategy β and the green ones for the combined approach (Strategy γ). The filled circles show the reduction of the peak load at the PCC if all 32 BESSs are integrated into the grid simultaneously.

The red crosses show the reduction if the BESS is operated with strategy α. It can be seen that the storage system reaches a reduction of the peak load at the associated node b in all 32 simulations. In most of the cases no peak load reduction at the PCC can be reached. The reason for this behavior is that in these cases the peaks in the load profile have a longer duration and thus the energy content is the limiting factor. As described in Section 3 and exemplary shown in Figure 4, the load profiles include reactive power, while the BESS in this study operates with active power only.

The initial motivation for a peak power tariff was to smooth out power peaks in the entire distribution grid. However, with this state-of-the-art peak shaving strategy only one case shows a reduction at the PCC. Even with all 32 storage systems integrated in the grid at the same time, only very small (13.63 kVA) improvements can be achieved with a conventional peak shaving algorithm.

The reduction for strategy β is marked with blue crosses. Since only one very high peak occurs at the PCC during the period under consideration, the change is almost identical with all 32 storage systems and corresponds to the maximum possible discharge power. Due to the fact that the BESS is located in different locations in the grid, line losses can be reduced during discharge. This results in relative reductions above one. However, for industrial customers themselves, the centralized algorithm never achieves a reduction in the peak load in this simulation setting.

The green crosses show the reduction if the BESS is operated in accordance to the newly developed combined approach (Strategy γ). In this case, both the local peak load and the global peak load will be reduced. It can be seen that the reduction at the location of the storage is nearly as high as with the state-of-the-art peak shaving strategy. However, a significant peak load reduction in the PCC is now also achieved. The filled circles in the figure show the reduction of the peak load at the PCC if all 32 BESSs are integrated into the grid simultaneously. Again, due to the fact that only one very high peak occurs at the PCC, the reduction with the centralized approach is almost the summed-up maximum possible discharge power of all BESSs. In contrast, with the combined approach with a reduction of 706.70 kVA, almost the same reduction is achieved as with the centralized approach (868.02 kVA).

Figure 7 supports the statements from the relative reduction plot by showing the absolute reduction for each simulation. The upper plot (a) shows the absolute peak load reduction for each simulation if the BESS is operated with strategy α. It can be seen that the peak reduction at the respective node b is minimum 5.05 kVA and maximum 53.3 kVA, which results with the numbers of Section 3.4 in an annual revenue of approximately $ 555.5 to $ 5,858.6. However, with this state-of-the-art peak shaving strategy only simulation 13 achieves a reduction at the PCC with 13.6 kVA. All others fail to reduce the peak load at the PCC. With the centralized approach (Strategy β), depicted in plot (b) the peak load at the PCC is reduced by 10.4 kVA to 83.1 kVA. The industrial consumers peak load is not reduced in any case, but is increased by up to 16.6 kVA in six cases.

The lower plot (c) shows the absolute peak load reduction for each simulation if the BESS is operated with strategy γ. The red bars show the difference in peak load at a local node b (=storage location), the blue bars show the peak load reduction at the PCC. The industrial consumers peak load reduction differs only in two cases above 1.0 kVA. The maximum occurs in simulation six with 2.8 kVA, which would result in a decreased annual revenue of $ 308.0. However, with this combined approach the peak load at the PCC is also reduced by 5.6 kVA to 56.7 kVA. Compared to the maximums before (53.3 kVA and 83.1 kVA), which both occurs at simulation six, the combined approach achieves a summed up reduction of 107.2 kVA. Integrating all 32 BESSs to the grid simultaneously, a reduction at the PCC of 706.7 kVA can be achieved.

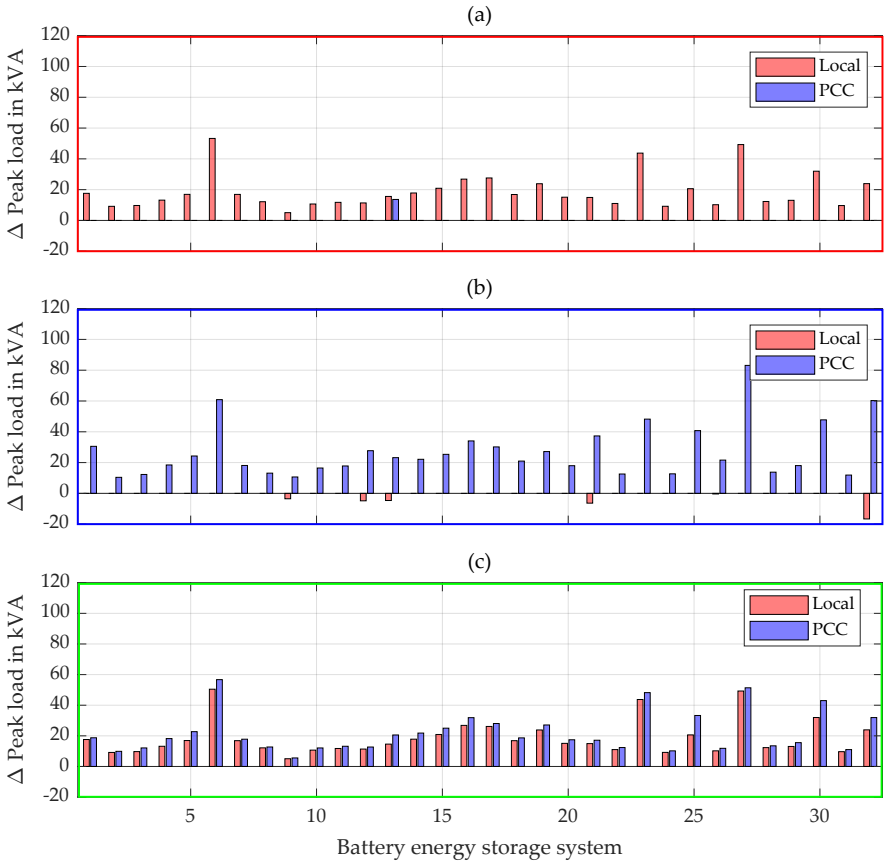

Figure 7. The upper plot (**a**) shows the absolute peak load reduction for each simulation if the battery energy storage system (BESS) is operated with strategy α. Plot (**b**) shows the results for the centralized approach (Strategy β). The lower plot (**c**) shows the absolute peak load reduction for each simulation if the BESS is operated with the newly developed combined approach (Strategy γ). The red bars show the difference in peak load at a local node b, the blue bars show the peak load reduction at the point of common coupling (PCC).

To evaluate the reduction in detail, the additional stress on the energy storage must also be considered. Figure 8 shows the results for all simulations using various key characteristics, which have been defined in a previous publication [14]. Subplot (a) shows the number of full equivalent cycles and the mean round-trip efficiency is displayed in subplot (b). The remaining characteristics describe the stress on the BESSs in greater detail. Subplot (c) shows the average cycle depth in discharge direction and the average resting time between two actions is illustrated in subplot (d). The number of alternations between charging and discharging (sign changes) per day is indicated in subplot (e), while subplot (f) shows the energy in relation to the BESS capacity that is charged or discharged between sign changes, respectively.

The highest peak at the PCC is 40.9 MVA and thus 1.4 MVA higher than the second highest peak. Consequently, all BESSs at the centralized approach (Strategy β) are only able to reduce this one maximum 15-minute peak and therefore only one sign change occurs. This also results in high resting times for the six month simulation period. Due to the losses in the storage system the total number of full equivalent cycles is 0.28 and consequently the cycle depth in discharge direction is 28% with a storage systems e^{rate} of one.

Comparing the results for strategy α and strategy γ, it can be seen that the BESSs have on average 1.2 full equivalent cycles more than the storage systems operating with a conventional peak shaving strategy. In the case of the LIB used, this results in a deviation in the remaining capacity of 0.01% (95.31 to 95.32) for the six month simulation period due to the high cycle stability. Resulting from very low additional stress on the storage system, there are hardly any differences for almost all other key characteristics. Only the duration

of the resting times between two actions falls significantly from 237.8 h to 131.3 h. However, this average resting time is still quite long and the storage systems remain underutilized with both strategies and it should be considered to use these to achieve additional revenues by using a multi-use approach [25]—a topic beyond the scope of this study.

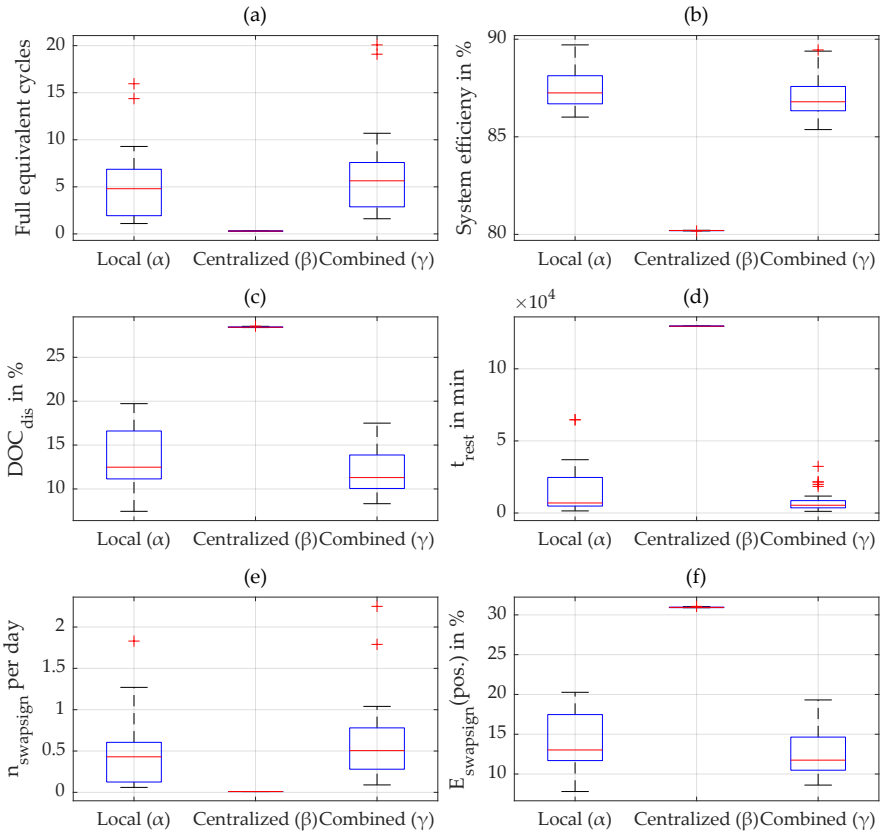

Figure 8. Detailed results about the additional stress on the battery energy storage systems (BESSs) for a six month simulation period. Subplot (**a**) shows the number of full equivalent cycles and the mean round-trip efficiency in % is displayed in subplot (**b**). Subplot (**c**) shows the average cycle depth in discharge direction in % and the average resting time in minutes between two actions is illustrated in subplot (**d**). The number of alternations between charging and discharging (sign changes) per day is indicated in subplot (**e**). Finally, subplot (**f**) shows the energy in relation to the BESS capacity that is charged between these sign changes.

5. Conclusions and Outlook

This paper presented a method to reduce the peak power at a specific node as well as at the transformer or PCC in distribution grids or microgrids by using BESSs. The storage systems are located at 32 various industrial consumers with individual load profiles in a MV-grid with 146 underlying LV-grids. A method of a combined operation strategy for BESSs located at industrial consumers has been developed to achieve both an improvement in the distribution grid as well as electricity bill savings for industrial consumers. By using and adapting the open_BEA framework, accurate co-simulations of BESSs and distribution grids are performed. The stress on the LIB-based stationary BESSs at the various strategies is evaluated by adapting the holistic energy storage simulation framework SimSES.

The newly developed combined approach (Strategy γ) uses a scaling factor for the power profile at the PCC in order to combine this load profile with the load profile of an individual industrial consumer. This combined profile serves as the input for the peak shaving operation strategy and the results are compared to a state-of-the-art peak shaving strategy (industrial consumer only; Strategy α) and a centralized approach (PCC only; Strategy β). The BESSs are economical optimally sized using a linear optimization approach.

Results show that with strategy γ both the local peak load and the global peak load can be reduced. The reduction at the location of the storage is nearly as high as with strategy α. With strategy γ the peak load at the PCC is reduced by 5.6 kVA to 56.7 kVA and the total reduction is always higher than with strategy α or strategy β. Although in this scenario the BESSs reduce both peaks, the additional stress for the six month simulation period is on average only 1.2 full equivalent cycles higher. This additional stress results in slightly higher aging (0.01%) with the used LIB.

Accelerated aging as well as adaptions in the energy management systems would have to be compensated financially by the grid operator to the storage owner or industrial consumer. However, it must be taken into account that the grid operator benefits economically by being able to avoid a possible grid reinforcement or transformer upgrade. The framework shown in this study requires communication (e.g., via the 5G communication standard [26,27] or the IEC 60870 standard [28]) between the grid operator and its current load at the PCC and the industrial consumer including the storage system. In addition, the algorithms introduced in this study require the creation of an economic and legal framework.

Future Work and Outlook

This study focuses on the technical potential of combined operation strategies for storage systems located at various industrial consumers in a distribution grid. The additional reduction in the peak load at the PCC may avoid the need of grid reinforcement or transformer exchange. Future work should focus on an economic analysis to compare the cost of installing a BESS with the costs of conventional grid reinforcement. From a grid perspective, future studies could also focus more on other grid-related applications as an additional service of the BESS, such as reactive power control.

Furthermore a highly discussed topic is the ecological assessment of storage systems. In addition to the economic assessment, it might also be worthwhile to perform an ecological analysis. This would allow a more precise comparison of the CO_2 impact of BESSs and the CO_2 impact caused by conventional grid reinforcement.

Author Contributions: D.K.: Conceptualization, Methodology, Software, Investigation, Writing—Original Draft L.S.: Methodology, Software, Formal analysis, Writing—Original Draft, Visualization N.C.: Methodology, Software, Writing—Review and Editing A.J.: Writing—Review and Editing, Supervision, Funding acquisition H.H.: Methodology, Writing—Review abd Editing, Supervision, Funding acquisition. All authors have read and agreed to the published version of the manuscript.

Funding: This publication was financially supported by the German Federal Ministry for Economic Affairs and Energy within the research project open_BEA (Grant No. 03ET4072), which is managed by Project Management Jülich. The responsibility for this study rests with the authors.

Institutional Review Board Statement: Not applicable.

Informed Consent Statement: Not applicable.

Data Availability Statement: Not applicable.

Conflicts of Interest: The authors declare no conflict of interest.

Parameters & variables

$E_t^{\text{actual,b}}$	actual energy content of a battery energy storage system at a specific node b for a specific time step t
$E_t^{\text{charge,b}}$	charged energy of a battery energy storage system at a specific node b for a specific time step t
$E_t^{\text{discharge,b}}$	discharged energy of a battery energy storage system at a specific node b for a specific time step t
$P_t^{\text{charge,b}}$	charging power of a battery energy storage system at a specific node b for a specific time step t
$P_t^{\text{discharge,b}}$	discharging power of a battery energy storage system at a specific node b for a specific time step t
P^{rated}	rated power of the power electronics
BESS_{tp}	energy throughput of a battery energy storage system
S_t^{b}	apparent power at a specific node b for a specific time step t
S_t^{comb}	combined apparent power including the power at a specific node b and the apparent power at the point of common coupling
$\text{S}^{\text{thresh,PCC}}$	peak shaving threshold power for a battery energy storage system operating with the grid-centered approach
$\text{S}^{\text{thresh,b}}$	peak shaving threshold power for a specific node b
$\text{S}^{\text{thresh,comb}}$	peak shaving threshold power for a battery energy storage system operating with the combined approach
σ_{b}	scaling factor: peak power at the point of common coupling in relation to the peak load at a specific node b
$\mathbf{S}^{\text{PCC}}$	vector of the apparent power at the point of common coupling for each time step t
$\mathbf{S}^{\text{Scaled,b}}$	scaled apparent power of the point of common coupling in relation to the peak load at a specific node b
$\mathbf{S}$	matrix for the apparent power at each node b for each time step t
e^{rate}	energy rate of the battery energy storage system
$\text{p}_{\text{BESS}}^{\text{invest}}$	storage investment costs per kWh
p_{peak}	annual peak demand charge per kVA
t_{proj}	project operation/depreciation period in years
w_{tp}	throughput penalty costs
η_{PE}	efficiency of the power electronics

Abbreviations

AC	alternating current

BESS	battery energy storage system
BMS	battery management system
C	carbon/graphite
DC	direct current
eDisGo	software for electric distribution grid optimization
LFP	lithium-iron-phosphate
LIB	lithium-ion battery
LV	low voltage
MV	medium voltage
open_BEA	open battery models for electrical grid applications
PCC	point of common coupling
SimSES	simulation of stationary energy storage systems
SOE	state of energy

Sets & indices

B	total number of nodes b in the distribution grid
H	time vector for the simulation period (time horizon)
T	time horizon
N	vector for all industrial consumers in the distribution grid
b	nodes with industrial consumers in the distribution grid
t	specific time step

References

1. Bollen, M.; Rönnberg, S. Hosting Capacity of the Power Grid for Renewable Electricity Production and New Large Consumption Equipment. *Energies* **2017**, *10*, 1325. [CrossRef]
2. Benetti, G.; Caprino, D.; Della Vedova, M.L.; Facchinetti, T. Electric load management approaches for peak load reduction: A systematic literature review and state of the art. *Sustain. Cities Soc.* **2016**, *20*, 124–141. [CrossRef]
3. Brinkel, N.; Schram, W.L.; AlSkaif, T.A.; Lampropoulos, I.; van Sark, W. Should we reinforce the grid? Cost and emission optimization of electric vehicle charging under different transformer limits. *Appl. Energy* **2020**, *276*, 115285. [CrossRef]
4. Nykvist, B.; Nilsson, M. Rapidly falling costs of battery packs for electric vehicles. *Nat. Clim. Chang.* **2015**, *5*, 329–332. [CrossRef]
5. Mehr, T.H.; Masoum, M.A.; Jabalameli, N. Grid-connected Lithium-ion battery energy storage system for load leveling and peak shaving. In Proceedings of the 2013 Australasian Universities Power Engineering Conference (AUPEC), Hobart, TAS, Australia, 29 September–October 2013; pp. 1–6. [CrossRef]
6. Oudalov, A.; Cherkaoui, R.; Beguin, A. Sizing and Optimal Operation of Battery Energy Storage System for Peak Shaving Application: 2007 IEEE Lausanne Power Tech. In Proceedings of the IEEE PowerTech, 2007 IEEE Lausanne, Lausanne, Switzerland, 1–5 July 2007; pp. 1–5. [CrossRef]
7. Mamun, A.; Narayanan, I.; Wang, D.; Sivasubramaniam, A.; Fathy, H.K. Multi-objective optimization of demand response in a datacenter with lithium-ion battery storage. *J. Energy Storage* **2016**, *7*, 258–269. [CrossRef]
8. Tiemann, P.H.; Bensmann, A.; Stuke, V.; Hanke-Rauschenbach, R. Electrical energy storage for industrial grid fee reduction—A large scale analysis. *Energy Convers. Manag.* **2020**, *208*, 112539. [CrossRef]
9. Martins, R.; Hesse, H.; Jungbauer, J.; Vorbuchner, T.; Musilek, P. Optimal Component Sizing for Peak Shaving in Battery Energy Storage System for Industrial Applications. *Energies* **2018**, *11*, 2048. [CrossRef]
10. Danish, S.M.S.; Ahmadi, M.; Danish, M.S.S.; Mandal, P.; Yona, A.; Senjyu, T. A coherent strategy for peak load shaving using energy storage systems. *J. Energy Storage* **2020**, *32*, 101823. [CrossRef]
11. Kucevic, D.; Englberger, S.; Sharma, A.; Trivedi, A.; Tepe, B.; Schachler, B.; Hesse, H.; Srinivasan, D.; Jossen, A. Reducing grid peak load through the coordinated control of battery energy storage systems located at electric vehicle charging parks. *Appl. Energy* **2021**, *295*, 116936. [CrossRef]
12. Naumann, M.; Truong, C.N.; Schimpe, M.; Kucevic, D.; Jossen, A.; Hesse, H.C. SimSES: Software for techno-economic Simulation of Stationary Energy Storage Systems. In *International ETG Congress 2017*; ETG-Fachbericht; VDE: Berlin/Offenbach, Germany, 2017; pp. 442–447.
13. Müller, U.P.; Schachler, B.; Scharf, M.; Bunke, W.D.; Günther, S.; Bartels, J.; Pleßmann, G. Integrated Techno-Economic Power System Planning of Transmission and Distribution Grids. *Energies* **2019**, *12*, 2091. [CrossRef]

14. Kucevic, D.; Tepe, B.; Englberger, S.; Parlikar, A.; Mühlbauer, M.; Bohlen, O.; Jossen, A.; Hesse, H. Standard battery energy storage system profiles: Analysis of various applications for stationary energy storage systems using a holistic simulation framework. *J. Energy Storage* **2020**, *28*, 101077. [CrossRef]
15. Murata. *Data Sheet of Sony Fortelion US26650FTC1 Battery Cell*; Murata: Kyoto, Japan, 2017.
16. Naumann, M.; Spingler, F.B.; Jossen, A. Analysis and modeling of cycle aging of a commercial $LiFePO_4$/graphite cell. *J. Power Sources* **2020**, *451*, 227666. [CrossRef]
17. Notton, G.; Lazarov, V.; Stoyanov, L. Optimal sizing of a grid-connected PV system for various PV module technologies and inclinations, inverter efficiency characteristics and locations. *Renew. Energy* **2010**, *35*, 541–554. [CrossRef]
18. German Federal Office of Justice. Stromnetzentgeltverordnung. (In German). Avaiable online: https://www.gesetze-im-internet.de/stromnev/BJNR222500005.html (accessed on 2 November 2021)
19. Tuunanen, J.; Honkapuro, S.; Partanen, J. Power-based distribution tariff structure: DSO's perspective. In Proceedings of the 2016 13th International Conference on the European Energy Market (EEM), Porto, Portuga, 6–9 June 2016; pp. 1–5. [CrossRef]
20. Collath, N.; Englberger, S.; Jossen, A.; Hesse, H. *Reduction of Battery Energy Storage Degradation in Peak Shaving Operation through Load Forecast Dependent Energy Management*; NEIS 2020, Ed.; VDE/ETG: Hamburg, Germany, 2020; pp. 1–6.
21. Mongird, K.; Viswanathan, V.; Balducci, P.; Alam, J.; Fotedar, V.; Koritarov, V.; Hadjerioua, B. An Evaluation of Energy Storage Cost and Performance Characteristics. *Energies* **2020**, *13*, 3307. [CrossRef]
22. Naumann, M.; Schimpe, M.; Keil, P.; Hesse, H.C.; Jossen, A. Analysis and modeling of calendar aging of a commercial LiFePO4/graphite cell. *J. Energy Storage* **2018**, *17*, 153–169. [CrossRef]
23. Vetter, J.; Novák, P.; Wagner, M.R.; Veit, C.; Möller, K.C.; Besenhard, J.O.; Winter, M.; Wohlfahrt-Mehrens, M.; Vogler, C.; Hammouche, A. Ageing mechanisms in lithium-ion batteries. *J. Power Sources* **2005**, *147*, 269–281. [CrossRef]
24. Figgener, J.; Stenzel, P.; Kairies, K.P.; Linßen, J.; Haberschusz, D.; Wessels, O.; Angenendt, G.; Robinius, M.; Stolten, D.; Sauer, D.U. The development of stationary battery storage systems in Germany—A market review. *J. Energy Storage* **2020**, *29*, 101153. [CrossRef]
25. Englberger, S.; Jossen, A.; Hesse, H. Unlocking the Potential of Battery Storage with the Dynamic Stacking of Multiple Applications. *Cell Rep. Phys. Sci.* **2020**, *1*. [CrossRef]
26. Gheisarnejad, M.; Khooban, M.H.; Dragicevic, T. The Future 5G Network-Based Secondary Load Frequency Control in Shipboard Microgrids. *IEEE J. Emerg. Sel. Top. Power Electron.* **2020**, *8*, 836–844. [CrossRef]
27. Garau, M.; Anedda, M.; Desogus, C.; Ghiani, E.; Murroni, M.; Celli, G. A 5G cellular technology for distributed monitoring and control in smart grid. In Proceedings of the 2017 IEEE International Symposium on Broadband Multimedia Systems and Broadcasting (BMSB), Cagliari, Italy, 7–9 June 2017; pp. 1–6. [CrossRef]
28. Hänsch, K.; Naumann, A.; Wenge, C.; Wolf, M. Communication for battery energy storage systems compliant with IEC 61850. *Int. J. Electr. Power Energy Syst.* **2018**, *103*, 577–586. [CrossRef]